AUT Journal of Modeling and Simulation

AUT J. Model. Simul., 54(2) (2022) 141-160
DOI: 10.22060/miscj.2022.21598.5291

Disturbance rejection of non-minimum phase MIMO systems: An iterative tuning approach

S. Tofighi[1]*, F. Merrikh-Bayat[2], F. Bayat[2]

[1] Department of Electrical Engineering, Amirkabir University of Technology (Tehran Polytechnic), Tehran, Iran
[2] Department of Electrical and Computer Engineering, University of Zanjan, Zanjan, Iran

ABSTRACT: An iterative tuning method is presented to obtain the multi-input multi-output (MIMO) feedforward controller coefficients to improve disturbance rejection in non-minimum phase (NMP) MIMO systems. In the NMP systems, eliminating the effect of disturbances may cause instability and also can impose extra costs to control the entire system. For this purpose, a simple feedforward controller structure is proposed. The unknown variables of the feedforward controller are calculated using LMIs such that the H∞ norm of the transfer function matrix from disturbance to output is minimized. By taking advantage of the frequency sampling techniques into account and using some iterative algorithms, a new tractable method is constructed to solve the problem. Also, a condition based on the right half plane (RHP) zero direction for the NMP system has been proposed to improve the disturbance rejection property of these systems. To obtain optimal coefficients, the algorithm is repeated several times to reach the best answer. The method employs convex techniques and CVX software to perform calculations. The efficiency of the method is shown in various practical examples using different performance indicators such as integral of absolute error (IAE), integral of squared error (ISE), integral of time multiplied by absolute error (ITAE), integral of time multiplied by squared error (ITSE).

Review History:

Received: Jul. 15, 2022
Revised: Nov. 25, 2022
Accepted: Dec. 10, 2022
Available Online: Feb. 28, 2023

Keywords:

non-minimum phase system
disturbance rejection
feedforward controller
linear matrix inequality
CVX

1- Introduction

Non-minimum phase behavior may appear in many industrial processes. Also, these systems often exhibit strong couplings between non-related inputs and outputs. Designing a feedforward controller could be a possible solution to reach control objectives. Disturbance rejection and control system design based on a high-order equivalent-input-disturbance estimator is presented in [1]. Disturbance rejection via feedforward compensation using an enhanced equivalent-input-disturbance approach is proposed in [2]. A stabilizing predictive controller with feedforward compensation for stable and time-delayed systems is given in [3]. An experimental evaluation of feedforward tuning rules is presented in [4]. In [5] comparison of additive and multiplicative feedforward control is presented. Disturbance attenuation using feedforward compensation for flight test results is studied in [6]. Transient response optimization in output regulation using feedforward selection is proposed in [7]. Disturbance rejection via feedforward compensation using an enhanced equivalent input disturbance approach is studied in [8]. Active disturbance rejection control based on a feedforward inverse system for turbofan engines is proposed in [9]. Performance, robustness, and noise amplification trade-offs in disturbance observer control design are presented in [10]. Data-driven design of a feedforward controller for rejecting measurable disturbance is studied in [11]. In [12] trajectory tracking and disturbance rejection control of random linear systems are presented. A controller synthesis method to achieve independent reference tracking performance and disturbance rejection performance is proposed in [13]. Also, the feedforward control technique has shown some applications in industries. Multivariable active disturbance rejection control for compression liquid chiller system is proposed in [14]. In [15] active disturbance rejection control for hydraulic systems with full-state constraints and input saturation is presented. In [16] a review of industrial feedforward control technology is given. Also, a new benchmark model for testing NMP systems is proposed in [17].

Linear matrix inequalities (LMI) are a way to solve many optimization and control problems and have been addressed in many studies. Designing MIMO controllers via LMIs especially for designing PIDs is the subject of many studies; see for example [18-22]. An important advantage of LMIs is that they are convex, and consequently, can be solved very effectively by using software/algorithms in polynomial time. Many problems in the field of control theory like stability analysis [23, 24], and calculating the H_∞ norm of a linear system transfer function [25], calculating the upper bound on μ [25], can be formulated using the LMI approach. An H_2/ H_∞ control design using LMI is presented in [26]. On the other hand, many other problems are non-convex and

*Corresponding author's email: saeedreza.tofighi@aut.ac.ir

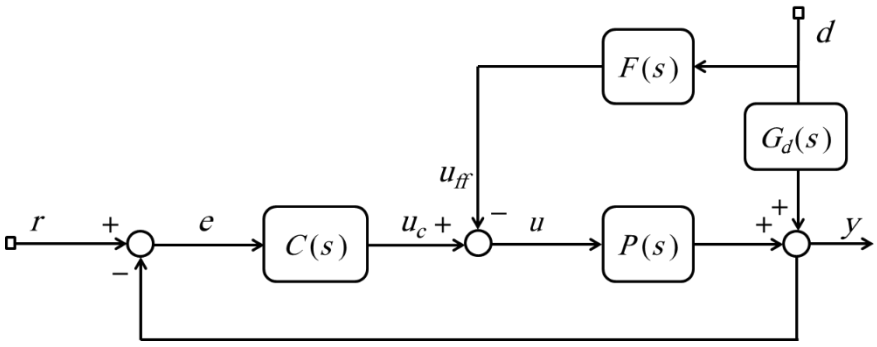

Fig. 1. The closed-loop system with a feedforward controller.

cannot be represented by LMIs. Hence, a large effort is made to cope with the non-convexity of these problems and to find approximate solutions using LMIs. Convex-concave decomposition and linearization methods are proposed in [27] to transform non-convex and bilinear matrix inequalities (BMI) into LMIs. For the first time, tuning of MIMO PIDs using the LMI approach is introduced in [18]. The main idea of this paper is to transform a MIMO PID controller design problem into static output feedback whose solution via the LMI approach was already known. Another considerable work in this field is [19]. In this paper, the MIMO PID controller is obtained by minimizing the low-frequency gain of the open-loop system subject to constraints on infinity norms of closed-loop transfer functions. In [22] the weighted sensitivity design of multivariable PID controllers for MIMO processes is presented. The main idea of this paper is to formulate the PID reference tracking problem into an H_∞ PID control problem by using the weighted sensitivity synthesis. Then, an iterative LMI algorithm has been developed to locally solve the optimal control problem.

In this paper, designing and tuning a MIMO feedforward controller is proposed to improve the disturbance rejection of NMP MIMO systems. The architecture consists of a MIMO feedforward controller from disturbance to the input of the plant. Each entry of the feedforward controller contains the first-order statement. These entries are considered to be stable and since the closed-loop system is stable, the entire system will be stable. This deals with the simple implementation of the feedforward controller. The unknown variables are calculated using LMIs such that the H_∞-norm of the transfer function matrix from disturbance to output is minimized. The proposed formulation to solve the problem is essentially non-convex and non-linear. By taking the advantage of the frequency sampling techniques into account and using some iterative algorithms such as a matrix extension of convex-concave decomposition, a new tractable method is constructed to solve the problem. We form the design problem with LMI restrictions in the frequency domain, and then we solve the problem to obtain the updated values of the variables. This method has an iterative nature which means that an initial point is required to begin the search. The search for the optimal or sub-optimal solution should begin with a stabilizing solution. This solution could be obtained from different methods or controllers proposed in papers. In each iteration, we replace the objective function and each constraint function with updated results to solve the minimization problem. The computations were carried out using the Matlab-based convex modeling framework CVX and iterated to convergence. Moreover, there may be problems that are not in the form of the constraints of this method, so finding a solution, if one exists, is not guaranteed. The proposed feedforward method could be extended to nonlinear systems using the method proposed in [28]. Also, to cope with the NMP effect of the system, an additional constraint is designed based on the RHP zero direction of the NMP system to improve the disturbance rejection property of these systems. Finally, some practical examples are performed to show the efficiency of the proposed feedforward method by comparing different performance indicators.

2- Proposed Control Structure

The proposed feedforward architecture of the closed-loop system is shown in Figure 1, where $r(t)$ is the reference input, $e(t)$ is the error, and d is a measurable output-referred plant disturbance. Signals $u(t)$ and $y(t)$ are the plant input and output, respectively. The plant, denoted as $P(s)$, is linear time-invariant and has m inputs (actuators) and p outputs (sensors). Also, there are at least as many actuators as plant outputs, which means that $p \le m$. The system is considered to be non-singular. The controller, $C(s)$, could be designed using any method. But this controller should guarantee stability and have a good set-point tracking performance. Also, this controller could partly reject disturbances. The feedforward controller is shown with $F(s)$.

A new structure for the MIMO feedforward controller is proposed in this paper. In this structure, each entry is considered a first-order transfer function. This is due to simplifying the tuning and implementation of the feedforward controller and also eliminating further complexity in computations. The structure of the feedforward controller is proposed as follows,

$$F = WX(WV)^{-1}, \tag{1}$$

where W is a weight function and a function of the Laplace variable, s, X is an unstructured matrix variable ,and V is a structured matrix variable. They are denoted for a two-input and two-output system in the following matrices,

$$W = \begin{bmatrix} s & 1 & 0 & 0 \\ 0 & 0 & s & 1 \end{bmatrix}, X = \begin{bmatrix} x_{11} & x_{12} \\ x_{21} & x_{22} \\ x_{31} & x_{32} \\ x_{41} & x_{42} \end{bmatrix}, \quad V = \begin{bmatrix} v_{11} & 0 \\ v_{21} & 0 \\ 0 & v_{32} \\ 0 & v_{42} \end{bmatrix}, \tag{2}$$

Thus, the feedforward controller is obtained in the following form

$$F(s) = \begin{bmatrix} \frac{x_{11}s + x_{21}}{v_{11}s + v_{21}} & \frac{x_{12}s + x_{22}}{v_{32}s + v_{42}} \\ \frac{x_{31}s + x_{41}}{v_{11}s + v_{21}} & \frac{x_{32}s + x_{42}}{v_{32}s + v_{42}} \end{bmatrix}. \tag{3}$$

The advantage of choosing first-order architecture is that investigating stability is easy for these systems since the closed-loop system is stable and if the feedforward controller is stable, the entire system stability is guaranteed. Also, the first-order feedforward controllers usually work well in practice.

3- Feedforward MIMO Controller Design

Designing a MIMO feedforward controller is proposed in this section to improve disturbance rejection property. For this purpose, the LMI method is employed to reach optimal satisfactory controllers. Consider Figure 1, the error of the system is in the following form,

$$E = -(I + PC)^{-1} PC\, R + (I + PC)^{-1}(G_d - PF)D, \tag{4}$$

here, consider $G_d(s)=I$, and $S = (I + PC)^{-1}$ is the *sensitivity* function. According to Eq. (4), for disturbance rejection, we should minimize $\bar{\sigma}[S(I - PF)]$. Therefore, our design problem is denoted in the following manner,

$$\begin{aligned} &\min t, && \text{(a)} \\ &s.t.\ \ \bar{\sigma}[(I + P(0)K_I)^{-1}(I - P(0)W(0)X(W(0)V)^{-1})] \le t, && \text{(b)} \\ &\bar{\sigma}[S(I - PWX(WV)^{-1})] \le S_{max},\ \forall \omega. && \text{(c)} \end{aligned} \tag{5}$$

Disturbance acts in low frequencies so our objective here is to minimize Eq. (5. b). Minimizing S, sensitivity function, in low frequencies leads to a peak of S in high frequencies. Also, the peak of S implies to overshoot in the time-domain response of the system. So, we minimize S such that the overshoot does not exceed the specified amount. Hence, the constraint of Eq. (5. c) is imposed on the design problem to limit the overshoot in the time-domain response of the system and also guarantee the whole system's stability. On the other hand, The PID controller, C, at low and near zero frequencies behaves like an integrator term, K_I.

The problem statement has some difficulties. This problem is not convex because the cost function and constraints are not affine expressions of the co-efficient. Also, it is not linear since matrix variables, X and V are multiplied by each other. Therefore, this problem statement is not in the form of LMI expression so we use a trick to approximately convert the problem to LMI form.

Also, consider $\bar{\sigma}[S(I - PWX(WV)^{-1})] < S_{max}$ for all ω's. This statement consists of an infinite number of constraints and this implies a semi-infinite constraint. Semi-infinite constraints could be handled by replacing them with a finite set of constraints at each of the given frequencies. For example, we use $\|S(i\omega_k)\|_\infty \le S_{max}$, $k = 1, \cdots, N$ instead of constraint $\|S\|_\infty \le S_{max}$ in Eq. (5. b). We will use subscripts to denote a transfer function evaluated at frequency $s = i\omega_k$. For example for a given complex matrix, the notation $P_k = P(i\omega_k)$ is used. The sampled problem is then obtained in the following form,

$$\begin{aligned} &\min t, && \text{(a)} \\ &s.t.\ \ \bar{\sigma}[(I + P(0)K_I)^{-1}(I - P(0)W(0)X(W(0)V)^{-1})] \le t, && \text{(b)} \\ &\bar{\sigma}[S_k(I - P_k W_k X(W_k V)^{-1})] \le S_{max}, \quad k = 1, \cdots, N. && \text{(c)} \end{aligned} \tag{6}$$

then to convert obtained sampled problem into LMI form, we should eliminate non-convexity and non-linearity difficulties. For this purpose, we defined the procedure in two steps.

Step 1: Constraint function 1

In the first step, the constraint function of Eq. (6. b) should be converted to an LMI form. Rearranging Eq. (6. b) gives,

$$\bar{\sigma}[(I+P(0)K_I)^{-1} (W(0)V-P(0)W(0)X) (W(0)V)^{-1}] \le t, \quad (7)$$

hence, we have,

$$\{S(W(0)V-P(0)W(0)X)\} \{(W(0)V)^{-1}(W(0)V)^{-*}\} \{(W(0)V-P(0)W(0)X)^* S^*\} \le t^2 I, \quad (8)$$

where for a complex matrix $Z \in C^{p\times q}$, Z^* is its (Hermitian) conjugate transpose. We used the notation $Z^{-*}=(Z^*)^{-1}$. The matrix inequality symbol $Z \preceq 0$ means that Z is Hermitian and negative semidefinite. Consider $Z_1 = S(W(0)V - P(0)W(0)X)$ and $A_1 = (W(0)V)^{-1}(W(0)V)^{-*}$; so, rearranging Eq. (8) results in the following form,

$$-t^2 I - Z_1(-A_1)Z_1^* \le 0, \quad (9)$$

therefore, using the Schur complement lemma we have,

$$\begin{bmatrix} -t^2 I & Z_1 \\ Z_1^* & -A_1^{-1} \end{bmatrix} \le 0, \quad (10)$$

we could write Eq. (10) in the following form,

$$\begin{bmatrix} -t^2 I & S(W(0)V-P(0)W(0)X) \\ (W(0)V-P(0)W(0)X)^* S^* & -(W(0)V)^*(W(0)V) \end{bmatrix} \le 0, \quad (11)$$

the term $(W(0)V)^*(W(0)V)$ is non-linear. Therefore, by simple manipulation and rearrangement of Eq. (11), we reach the following form,

$$\begin{bmatrix} -t^2 I & S(W(0)V-P(0)W(0)X) \\ (W(0)V-P(0)W(0)X)^* S^* & 0 \end{bmatrix} \le \begin{bmatrix} 0 & 0 \\ 0 & (W(0)V)^*(W(0)V) \end{bmatrix}, \quad (12)$$

to linearize non-linear terms according to the approximate linearization of quadratic matrix inequalities (QMI) from [19], we can write $(W(0)V)^*(W(0)V) \ge (W(0)V)^*(W(0)\tilde{V}) + (W(0)\tilde{V})^*(W(0)\tilde{V}) - (W(0)\tilde{V})^*(W(0)\tilde{V})$. Where $\tilde{V}$ is an arbitrary matrix of suitable dimension. Therefore, by manipulating and rearranging Eq. (12) we have

$$\Phi_1 = \left[\begin{array}{c|c} -t^2 I & S(W(0)V-P(0)W(0)X) \\ \hline (W(0)V-P(0)W(0)X)^* S^* & \begin{array}{c} -(W(0)V)^*(W(0)\tilde{V}) \\ -(W(0)\tilde{V})^*(W(0)V) \\ +(W(0)\tilde{V})^*(W(0)\tilde{V}) \end{array} \end{array}\right] \le 0 \quad (13)$$

The constraint function is now in the form of an LMI. Because Φ_1 is real and does not have an imaginary part, we can directly use Eq. (13) in simulation.

Step 2: Constraint function 2

In this step, the constraint function shown by Eq. (6. c) should be converted into LMI form by making non-convex terms into convex expressions and linearizing non-linear terms. Rearranging Eq. (6. c) gives,

$$\bar{\sigma}\left[S_k(W_kV - P_kW_kX)(W_kV)^{-1}\right] \le S_{max}, \quad (14)$$

then, we have,

$$\{S_k(W_kV-P_kW_kX)\}\{(W_kV)^{-1}(W_kV)^{-*}\} \{(W_kV-P_kW_kX)^* S_k^*\} \le S_{max}^2 I, \quad (15)$$

consider $Z_2 = S_k(W_kV - P_kW_kX)$ and $A_2 = (W_kV)^{-1}(W_kV)^{-*}$. Rearranging Eq. (15) results in the following form,

$$-S_{max}^2 I - Z_2(-A_2)Z_2^* \le 0, \quad (16)$$

by using the Schur complement lemma we have,

$$\begin{bmatrix} -S_{max}^2 I & Z_2 \\ Z_2^* & -A_2^{-1} \end{bmatrix} \le 0, \quad (17)$$

Eq. (17) can be written in the following form,

$$\begin{bmatrix} -S_{max}^2 I & S_k(W_kV-P_kW_kX) \\ (W_kV-P_kW_kX)^* S^* & -(W_kV)^*(W_kV) \end{bmatrix} \le 0, \quad (18)$$

the term $(W_kV_1)^*(W_kV_1)$ is nonlinear. So, by simple rearrangement of Eq. (18), we have,

$$\begin{bmatrix} -S_{max}^2 I & S_k\left(W_k V - P_k W_k X\right) \\ \left(W_k V - P_k W_k X\right)^* S^* & 0 \end{bmatrix} \leq \begin{bmatrix} 0 & 0 \\ 0 & \left(W_k V\right)^* \left(W_k V\right) \end{bmatrix}, \tag{19}$$

as mentioned before the non-linear term of Eq. (19) should be linearized. To do this $(W_k V)^*(W_k V) \geq (W_k V)^*(W_k \tilde{V}) + (W_k \tilde{V})^*(W_k V) - (W_k \tilde{V})^*(W_k \tilde{V})$ could be used. Therefore, simple manipulation gives,

$$\Phi_2 = \left[\begin{array}{c|c} -S_{max}^2 I & S_k\left(W_k V - P_k W_k X\right) \\ \hline \left(W_k V - P_k W_k X\right)^* S^* & \begin{array}{l} -(W_k V)^*(W_k \tilde{V}) - (W_k \tilde{V})^*(W_k V) \\ +(W_k \tilde{V})^*(W_k \tilde{V}) \end{array} \end{array}\right] \leq 0, \tag{20}$$

since Eq. (20) has imaginary terms, we should use the following form to use obtained results in simulation,

$$\Phi_3 = \begin{bmatrix} Re(\Phi_2) & Im(\Phi_2) \\ -Im(\Phi_2) & Re(\Phi_2) \end{bmatrix} \leq 0 \tag{21}$$

so, we can use Eq. (21) directly in simulation.

Again, consider our design problem denoted by Eq. (5. b) and Eq. (5. c). We could restate this design problem using the LMI form obtained in Eq. (13) and Eq. (21). Therefore, the design problem is obtained in the following form,

$$\begin{aligned} &min\, t, && \text{(a)} \\ &s.t. \quad \Phi_1 \leq t, && \text{(b)} \\ &\Phi_{3k} \leq 0, \quad k = 1, \cdots, N && \text{(c)} \end{aligned} \tag{22}$$

Now we can directly use Eq. (22. b) and Eq. (22. c) in simulations to find an optimal feedforward controller to improve disturbance rejection of the system.

4- Feedforward controller design for NMP systems

In this section, designing an additional constraint for the design problem of Eq. (22) is proposed to improve the disturbance rejection property of NMP MIMO systems. For this purpose, a matrix of disturbances denoted with, G_d, is considered here; where each vector of this matrix is a scalar disturbance. Considering Fig. 1 and Eq. (4), the relation between *e* to *d* by factoring G_d is as follows

$$E = S\left[I - PFG_d^{-1}\right]G_d D \tag{23}$$

by considering $S_d = \left[I - PFG_d^{-1}\right]$; Eq. (23) could be written in the following form

$$E = SS_d G_d D \tag{24}$$

so, the performance objective is then satisfied if

$$\left\|SS_d G_d\right\|_2 = \bar{\sigma}\left(SS_d G_d\right) < 1 \ \forall\omega \ \Leftrightarrow \ \left\|SS_d G_d\right\|_\infty < 1 \tag{25}$$

The disturbance direction is defined as $y_d = \left\|G_d\right\|_2^{-1} G_d$ [25]. By using this definition and some manipulation we have:

$$\left\|SS_d y_d\right\|_2 < \left\|G_d\right\|_2^{-1} \ \forall\omega \tag{26}$$

Eq. (25) and Eq. (26) are equivalent. Also, Eq. (26) shows that S must be less than $\left\|G_d\right\|_2^{-1}$ only in the direction of y_d. Where y_d is the disturbance output $y_d = G_d d$.

Now, if the system has an RHP zero at $s = z$ then the performance may be poor when the disturbance is aligned with the output direction of this zero. To see this use $y_z^H S(z) = y_z^H$ and apply the maximum modulus principle to $f(s) = y_z^H S G_d$. Also, by considering $\hat{G}_d = S_d G_d$; the following relation could be obtained, which will be used in designing a condition to improve disturbance rejection for NMP MIMO systems

$$\left\|S\hat{G}_d\right\|_\infty \geq \left|y_z^H \hat{G}_d(z)\right| = \left|y_z^H y_d\right| . \left\|\hat{G}_d(z)\right\|_2 \tag{27}$$

where, y_z is the direction of the RHP zero and y_z^H denotes its Hermitian. To satisfy $\left\|S\hat{G}_d\right\|_\infty < 1$, we must have at least the following requirement for a given disturbance d

$$\left|y_z^H \hat{G}_d(z)\right| < 1 \tag{28}$$

Now, we should consider the obtained condition of Eq. (28) in designing a feedforward controller. For this purpose, consider $F = WX\left(WV\right)^{-1}$. So, we have

$$\begin{bmatrix} y_{d1} \\ y_{d2} \end{bmatrix} = G_d \begin{bmatrix} d_1 \\ d_2 \end{bmatrix} = \begin{bmatrix} g_{d1} & g_{d2} \end{bmatrix} \begin{bmatrix} d_1 \\ d_2 \end{bmatrix} \tag{29}$$

Eq. (29) shows the effect of a scalar disturbance on the outputs. Again consider Eq. (28), where $\hat{G}_d = G_d - PF$. Then we have

$$\hat{G}_d = G_d - P\left[WX(WV)^{-1}\right] \tag{30}$$

Our aim here is to convert the condition of Eq. (28) into the proper form of a LMI function. Eq. (28) could be written in the following form

$$\begin{cases} y_z^H \hat{G}_d(z) < 1 \\ -y_z^H \hat{G}_d(z) < 1 \end{cases} \tag{31}$$

consider $y_z^H \hat{G}_d(z) < 1$, to convert into LMI form

$$G_d - PF < 1 \tag{32}$$

hence, we have

$$G_d - PWX(WV)^{-1} < 1 \tag{33}$$

by multiplying (WV) into both sides of the non-equality of Eq. (33), we get

$$G_d(WV) - PWX < WV \tag{34}$$

so, we have

$$G_d(WV) - PWX - WV < 0 \tag{35}$$

Eq. (35) is multiplied by y_z^H,

$$y_z^H\left[G_d(WV) - PWX - WV\right] < 0 \tag{36}$$

Also, condition $-y_z^H \hat{G}_d(z) < 1$ in Eq. (31), could be converted into LMI form using a similar procedure.

By applying the condition of Eq. (36) to the feedforward design problem shown by Eq. (22), we can improve the disturbance rejection property of NMP MIMO systems. The efficiency of implementing the proposed method for NMP MIMO systems is investigated in the simulations.

5- Numerical examples

In this section, two numerical examples are performed to show the efficiency of the proposed feedforward method designed to improve disturbance rejection of NMP systems. The computations were carried out using the Matlab-based convex modeling framework CVX [30] using the SDPT3 4.0 software [31] for solving the semidefinite program (SDP). Here, we used a Corei5 laptop with 4GB RAM for computations.

Example 1: The plant considered here is a simplified model of the classic two-input two-output Woodberry binary distillation column described in [32]. The plant transfer function is in the following form,

$$P_1(s) = \begin{bmatrix} \dfrac{12.8}{16.7s+1} & \dfrac{-18.9}{21s+1} \\ \dfrac{6.6}{10.9s+1} & \dfrac{-19.4}{14.2s+1} \end{bmatrix}, \tag{37}$$

Each entry in this plant is a first-order transfer function. The dynamics are quite coupled, so finding a good MIMO PID controller is not simple. The main controller used here is a PID controller obtained in the following form using the method proposed in [19],

$$\begin{aligned} K_p &= \begin{bmatrix} 0.4401 & -0.4787 \\ 0.2105 & -0.2829 \end{bmatrix}, \\ K_i &= \begin{bmatrix} 0.0099 & -0.0097 \\ 0.0031 & -0.0068 \end{bmatrix}, \\ K_d &= \begin{bmatrix} -0.0007 & 0.0058 \\ 0.0005 & -0.0040 \end{bmatrix}, \end{aligned} \tag{38}$$

by considering obtained PID controller, the MIMO feedforward controller transfer function derived using the proposed LMI approach is obtained in the following form,

$$F(s) = \begin{bmatrix} \dfrac{19.72s+0.9617}{s+6.126} & \dfrac{-10.62s-0.8911}{s+5.826} \\ \dfrac{9.019s+0.3272}{s+6.126} & \dfrac{-9.022s-0.6035}{s+5.826} \end{bmatrix}, \tag{39}$$

System results in 22 iterations and a total CPU time of 11.97 s. According to the obtained results, the proposed feedforward controller acts satisfactorily. As could be observed in Figure 2, disturbance rejection and tracking are significantly improved. Also, control signals and root mean square (RMS) of the control signal is derived in Figure 3, 4, and 5, respectively. Table 1 is performed to compare the efficiency of the proposed method using different performance indices. This table is performed to investigate its efficiency for disturbance rejection. Also, to compare results different performance parameters are considered in Table 1. For the error signal, the common integral performance function types IAE, ISE, ITAE, and ITSE are used to compare results in each channel, separately. The results of Table 1 verify that our method works well for the considered objectives.

Example 2: Consider the following non-minimum phase system,

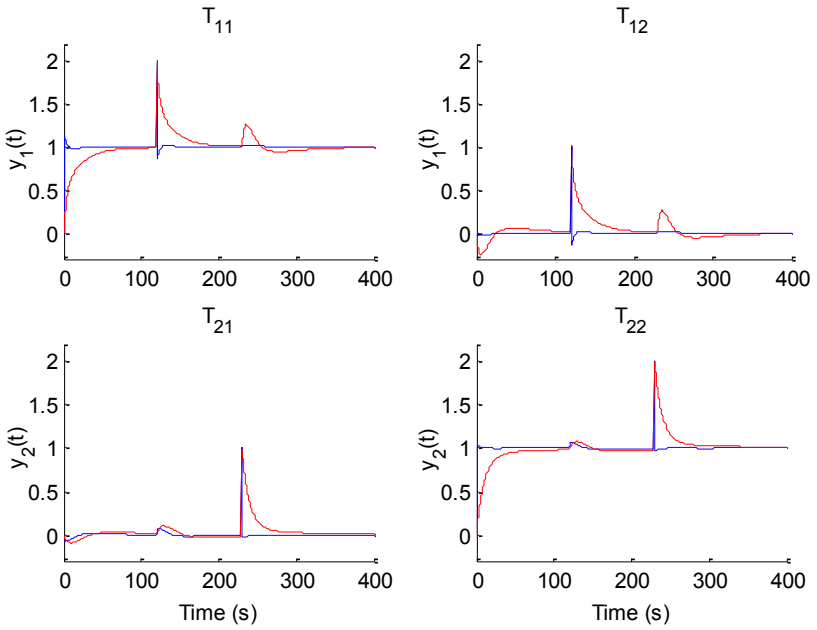

Fig. 2. Comparison between the closed-loop step response from r to y for the MIMO system without feedforward controller (red line) and with feedforward controller (blue line).

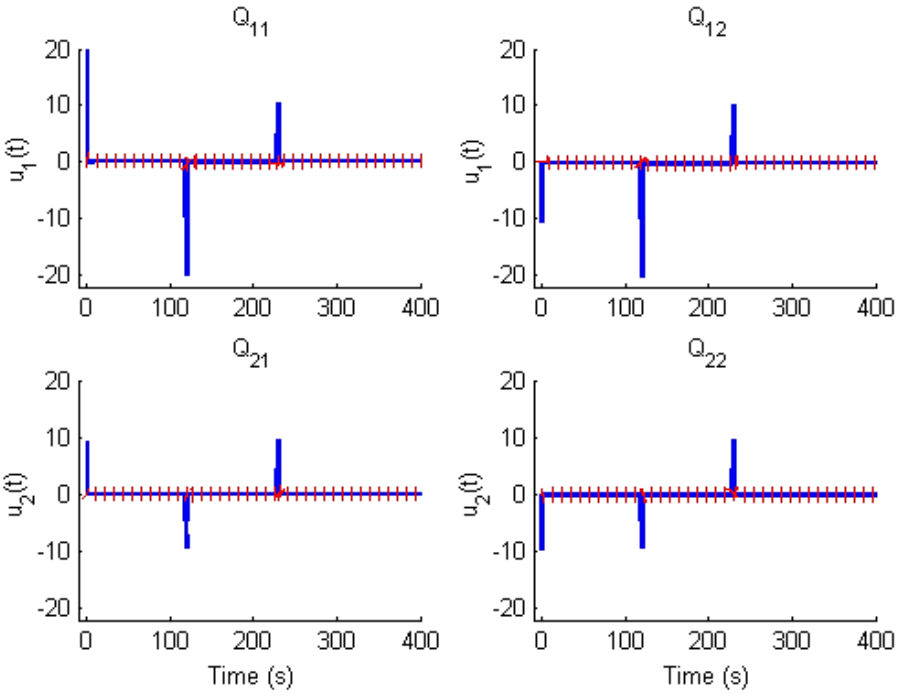

Fig. 3. Control signals without (red line) and with (blue line) employing the feedforward controllers.

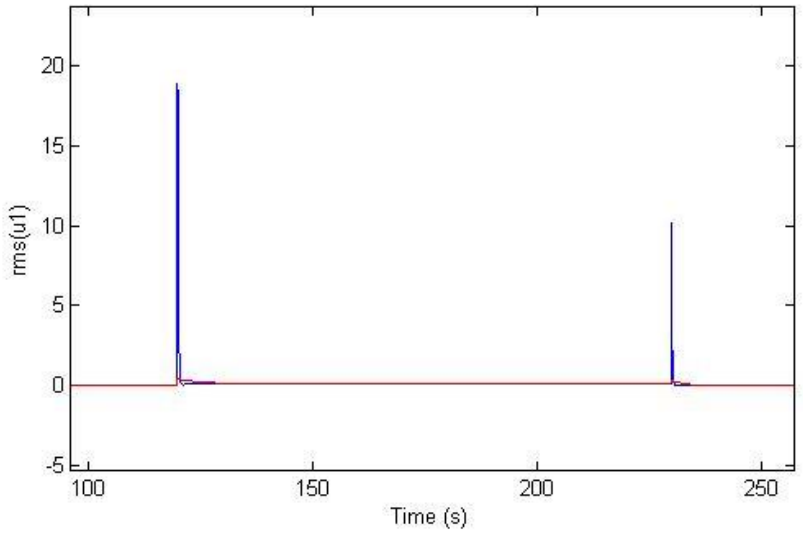

Fig. 4. Comparison between RMS of control signals for the NMP MIMO system with feedforward controller (blue line) and without feedforward controller (red line) for channel 1.

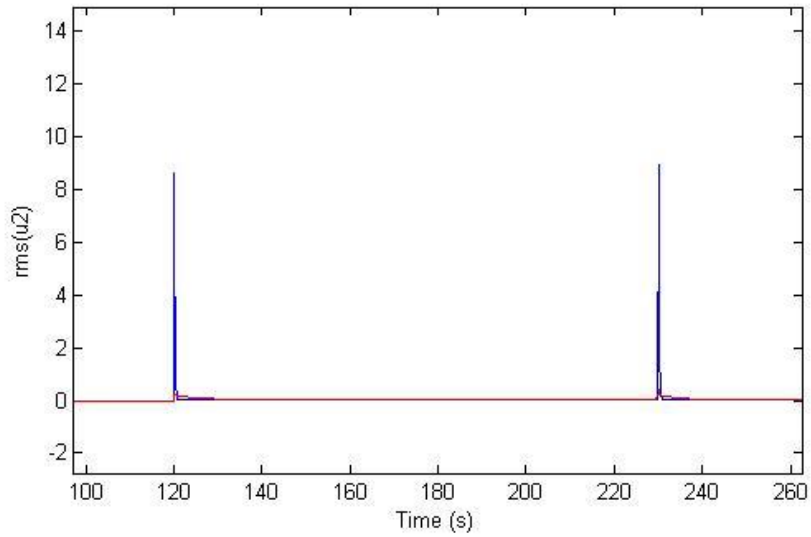

Fig. 5. Comparison between RMS of control signals for the NMP MIMO system with feedforward controller (blue line) and without feedforward controller (red line) for channel 2.

Table 1. Comparison between closed-loop performance indices with and without using the proposed feedforward controller for disturbance rejection property.

System	Error No.	IAE	ISE	ITAE	ITSE
With Feedforward	e_1	1.87	0.11	3.74×10^2	0.2104×10^4
Without Feedforward	e_1	21.38	5.98	39.88×10^2	13.775×10^4
With Feedforward	e_2	2.15	0.13	3.77×10^2	0.5442×10^4
Without Feedforward	e_2	16.96	5.30	40.07×10^2	29.156×10^4

$$P_2(s)=\begin{bmatrix}\dfrac{8}{16s+1} & \dfrac{-18}{9s+9}\\ \dfrac{6}{12s+6} & \dfrac{-25}{15s+1}\end{bmatrix}, \tag{40}$$

This system has an RHP zero at s =7.078. The main controller used here is a PID controller obtained in the following form using the method proposed in [19],

$$\begin{aligned}K_p&=\begin{bmatrix}0.2099 & -0.1005\\ 0.0191 & -0.1526\end{bmatrix},\\ K_i&=\begin{bmatrix}0.0234 & 0.0138\\ 0.0016 & -0.0136\end{bmatrix},\\ K_d&=\begin{bmatrix}0.0001 & -0.0021\\ 0.0028 & 0.0006\end{bmatrix},\end{aligned} \tag{41}$$

the output zero direction for this system is

$$y_z^H=[-0.6858 \quad 0.7278] \tag{42}$$

which shows that the RHP zero mostly affects the second channel of the system. By considering obtained PID controller, the feedforward MIMO controller transfer function derived using the LMI approach is obtained in the following form,

$$F(s)=\begin{bmatrix}\dfrac{2.063s+0.2211}{s+1.751} & \dfrac{-0.2811s-0.01843}{s+1.824}\\ \dfrac{0.08353s+0.008844}{s+1.751} & \dfrac{-0.609s-0.0737}{s+1.824}\end{bmatrix}, \tag{43}$$

This system results in 26 iterations and total CPU time 8.26 s. As it could be observed in Figure 6 and Figure 7, disturbance rejection is significantly improved. Control signals are derived in Figure 8, and 9 and the RMS of control signals are given in Figure 10 and 11. Also, comparison between singular values of the NMP system with and without feedforward controller is shown in Figure 12. To compare results, ISE performance parameter is considered in Figure 13 to compare results in each channel, separately. Results of Figure 13 verify that our method works well for the considered objectives.

Example 3: The following transfer matrix was proposed in [33] as a benchmark system whose appropriate input-output pairing cannot be determined effectively using the relative gain array (RGA):

$$P_3(s)=\frac{1-s}{(5s+1)^2}\begin{bmatrix}1 & -4.19 & -25.96\\ 6.19 & 1 & -25.96\\ 1 & 1 & 1\end{bmatrix} \tag{44}$$

This transfer matrix has three NMP transmission zeros at s = 1. The gains of the MIMO PI controller are obtained as follows [34]

$$\begin{aligned}K_p&=\begin{bmatrix}0.0821 & 0.0260 & 0.6753\\ -0.2996 & 0.2071 & -0.6095\\ 0.0211 & -0.0601 & 0.2449\end{bmatrix},\\ K_i&=\begin{bmatrix}0.0022 & 0.0012 & 0.0302\\ -0.0136 & 0.0099 & -0.0252\\ 0.0002 & -0.0003 & 0.0021\end{bmatrix}\end{aligned} \tag{45}$$

Assuming the above PI controller in the loop and considering the initial condition as follows

$$\tilde{y}=\left[\begin{array}{c|c|c|c|c|c}1 & 1 & 0 & 0 & 0 & 0\\ \hline 0 & 0 & 1 & 1 & 0 & 0\\ \hline 0 & 0 & 0 & 0 & 1 & 1\end{array}\right]^T \tag{46}$$

The proposed design procedure results in the following

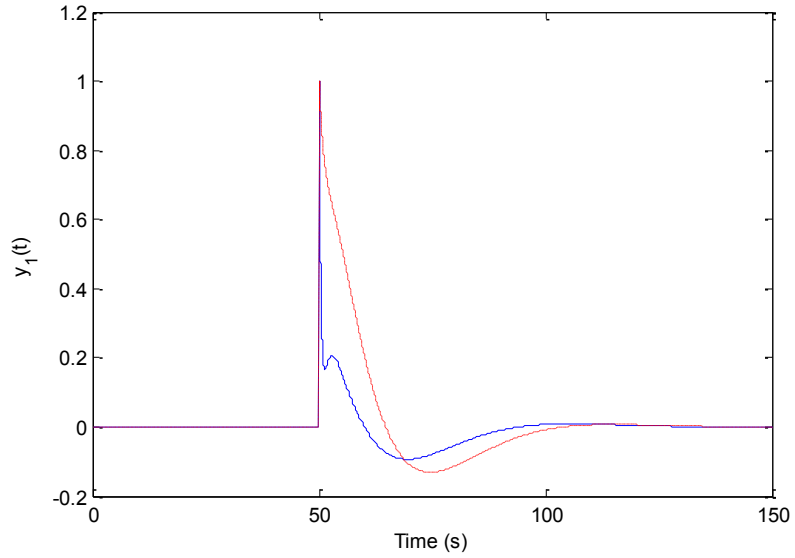

Fig. 6. Comparison between disturbance rejection for the NMP MIMO system with feedforward controller (blue line) and without feedforward controller (dashed-dotted red line) for channel 1.

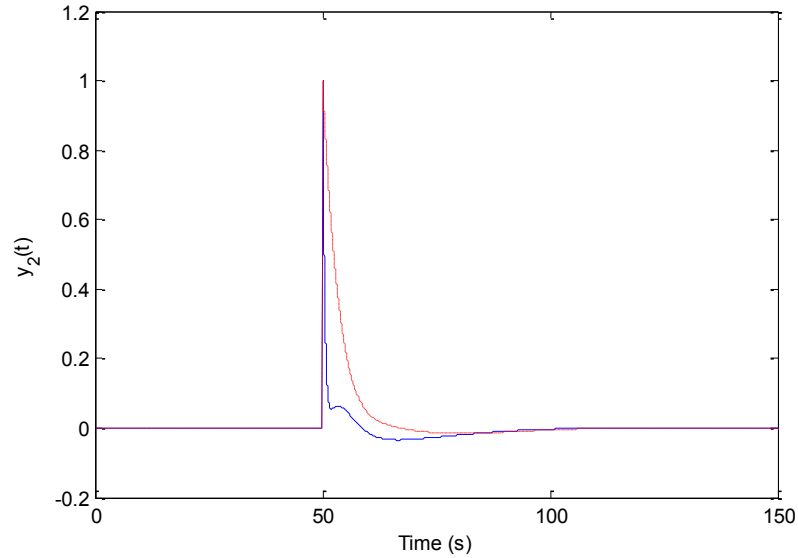

Fig. 7. Comparison between disturbance rejection for the NMP MIMO system with feedforward controller (blue line) and without feedforward controller (dashed-dotted red line) for channel 2.

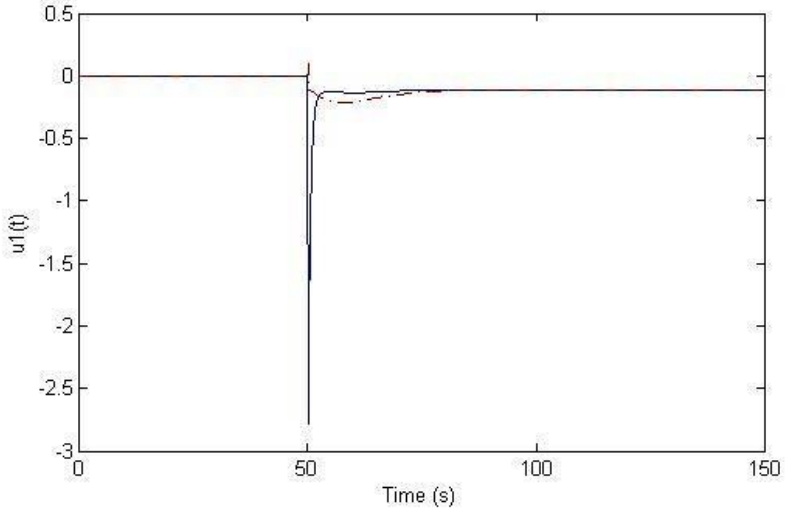

Fig. 8. Comparison between control signals for the NMP MIMO system with feedforward controller (blue line) and without feedforward controller (dashed-dotted red line) for channel 1.

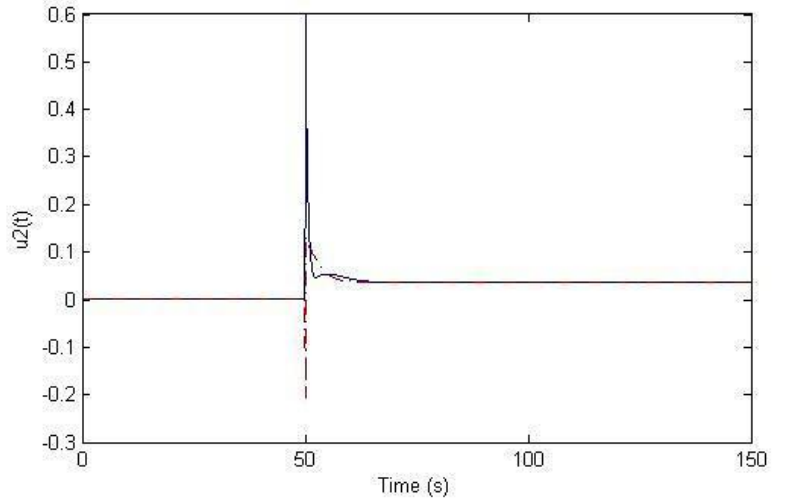

Fig. 9. Comparison between RMS of control signals for the NMP MIMO system with feedforward controller (blue line) and without feedforward controller (red line) for channel 2.

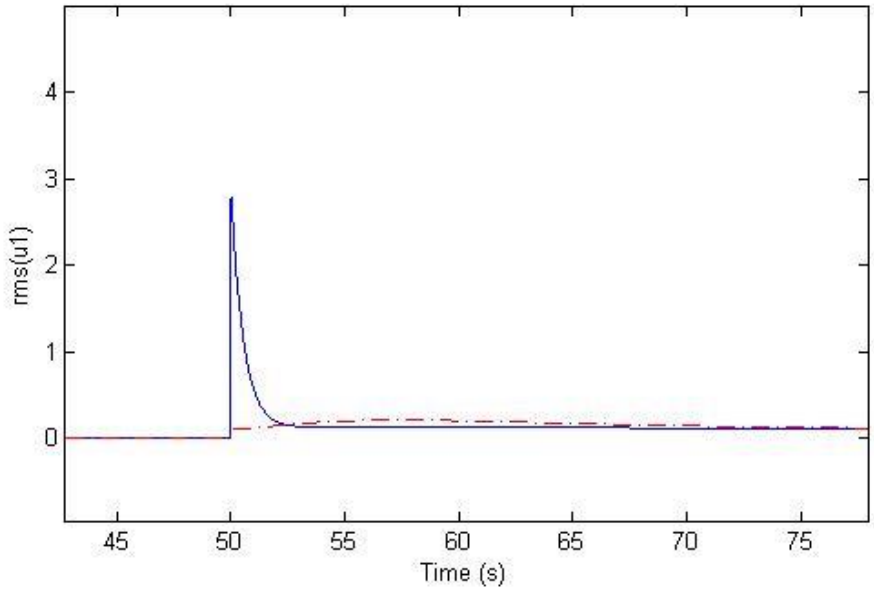

Fig. 10. Comparison between RMS of control signals for the NMP MIMO system with feedforward controller (blue line) and without feedforward controller (dashed-dotted red line) for channel 1.

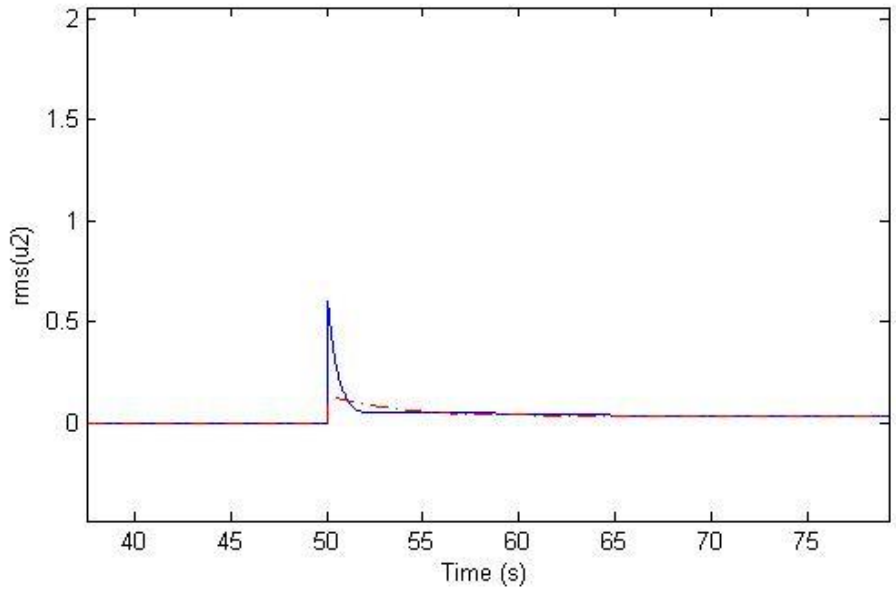

Fig. 11. Comparison between RMS of control signals for the NMP MIMO system with feedforward controller (blue line) and without feedforward controller (dashed-dotted red line) for channel 2.

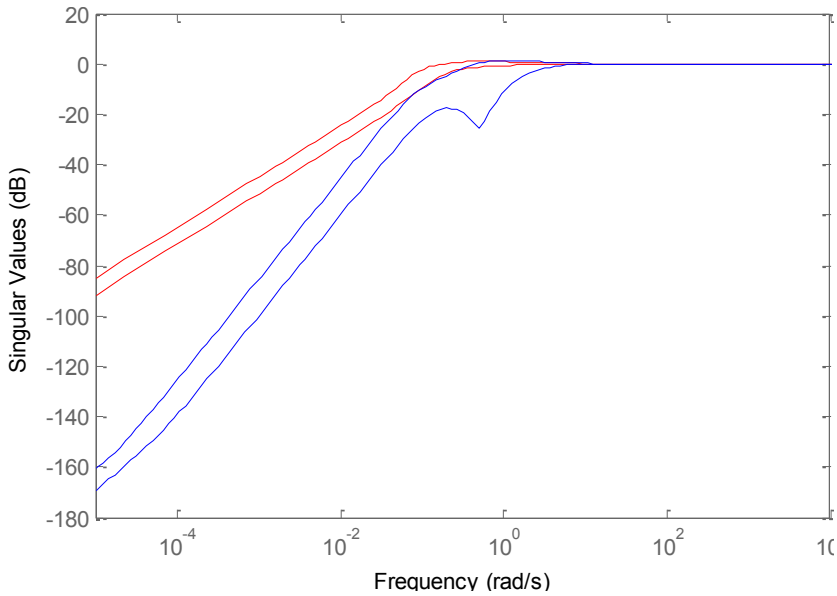

Fig. 12. Comparison between singular values of NMP MIMO system with feedforward controller (blue line) and without feedforward controller (red line).

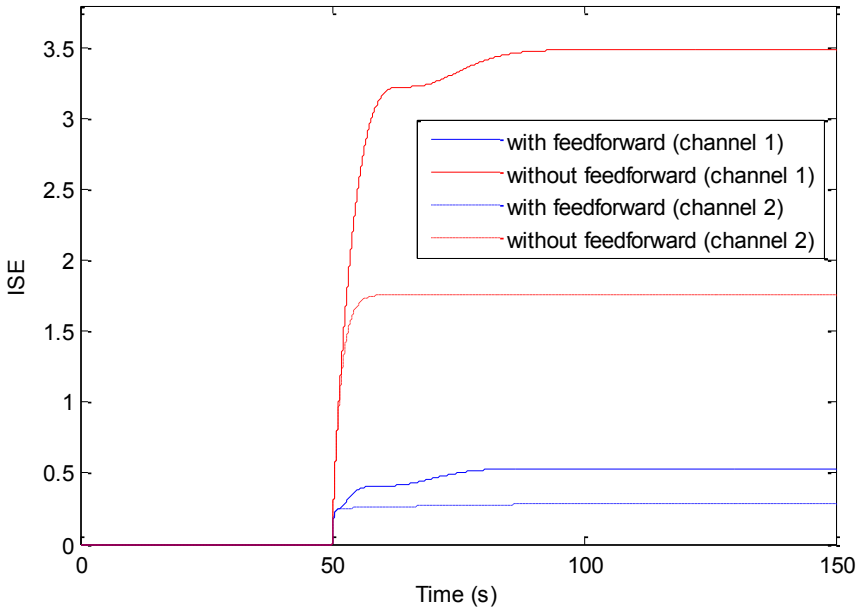

Fig. 13. Comparison between closed-loop performance indices (ISE criterion) with feedforward (blue line) and without feedforward (red line).

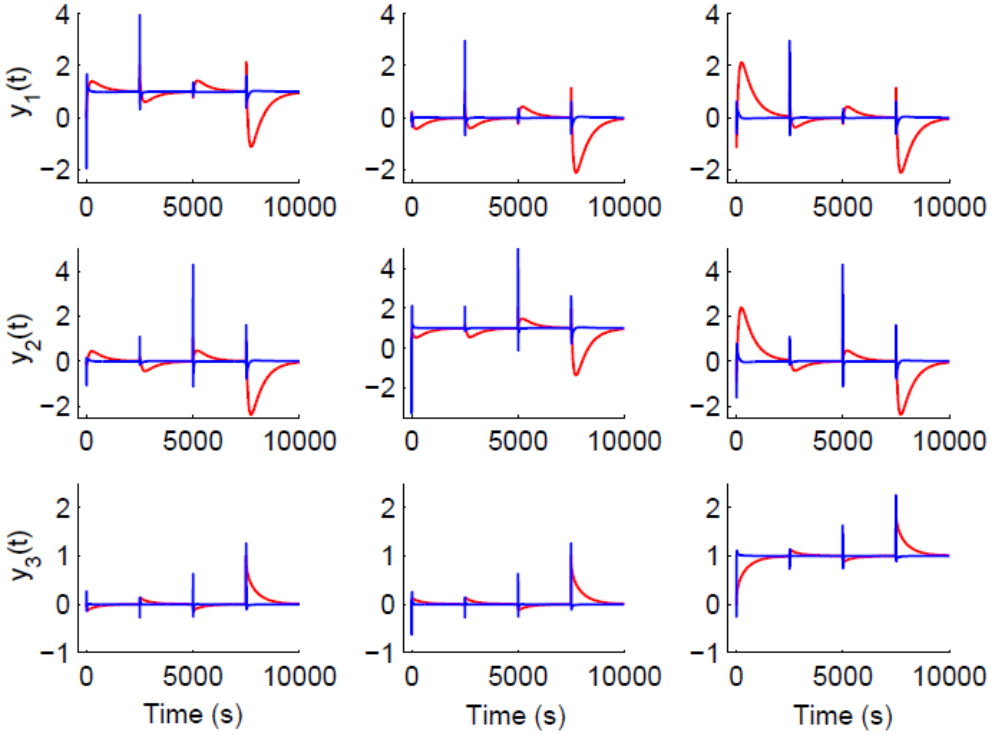

Fig. 14. Closed-loop step responses without (red line) and with (blue line) employing the feedforward controllers

feedforward MIMO controllers

$$F(s)=\begin{bmatrix} \frac{1.789s+4.679}{s+4.675} & \frac{4.289s-3.785}{s+4.683} & \frac{-36.68s+9.713}{s+1.942} \\ \frac{20.75s-5.58}{s+4.675} & \frac{-28.54s+4.687}{s+4.683} & \frac{31.05s-9.713}{s+1.942} \\ \frac{1.468s+0.9008}{s+4.675} & \frac{4.988s-0.9023}{s+4.683} & \frac{-7.159s+1.942}{s+1.942} \end{bmatrix} \quad (47)$$

This system results in 23 iterations and a total CPU time of 13.44 s. As could be observed in Figure 14, disturbance rejection and set-point tracking are improved by exerting the feedforward controllers. In this figure, the closed-loop step response of the system with and without the dual-feedforward MIMO method is considered. Also, the results of Table 2 confirm that our method acts well for disturbance rejection. Figure 15 shows the disturbance rejection property of each channel separately with and without feedforward controllers. Also, the disturbance rejection property of the proposed method for three different feedforward controllers obtained by using three different initial conditions is shown in Figure 16. In this figure, the blue, black, and red plots correspond to the controllers obtained by using the initial conditions $\tilde{y}_1 = 1\tilde{y}$, $\tilde{y}_2 = 5\tilde{y}$ and $\tilde{y}_3 = 10\tilde{y}$, respectively. Also, control signals are derived in Figure 17. The RMS of control signals is given in Figures 18, 19, and 20 for channels 1 to 3, respectively. The results show that our proposed method converges with different initial conditions and it is not very sensitive to the initial condition used for controller design.

6- Conclusion

In this paper, we introduced a feedforward controller for NMP MIMO systems to improve disturbance rejection properties. For this purpose, an LMI approximation is proposed for generally non-convex systems. This method is naturally iterative and the results show that it works well for the considered objectives. Structured and unstructured variable matrices are used in designing the feedforward controller. Also, to cope with the NMP effect of the system, a condition is designed based on the RHP zero direction of the NMP system to improve the disturbance rejection property. Finally, the simulations revealed that the proposed method shows satisfactory results. Therefore, it is expected that this leads to satisfactory results in dealing with a wide variety of problems.

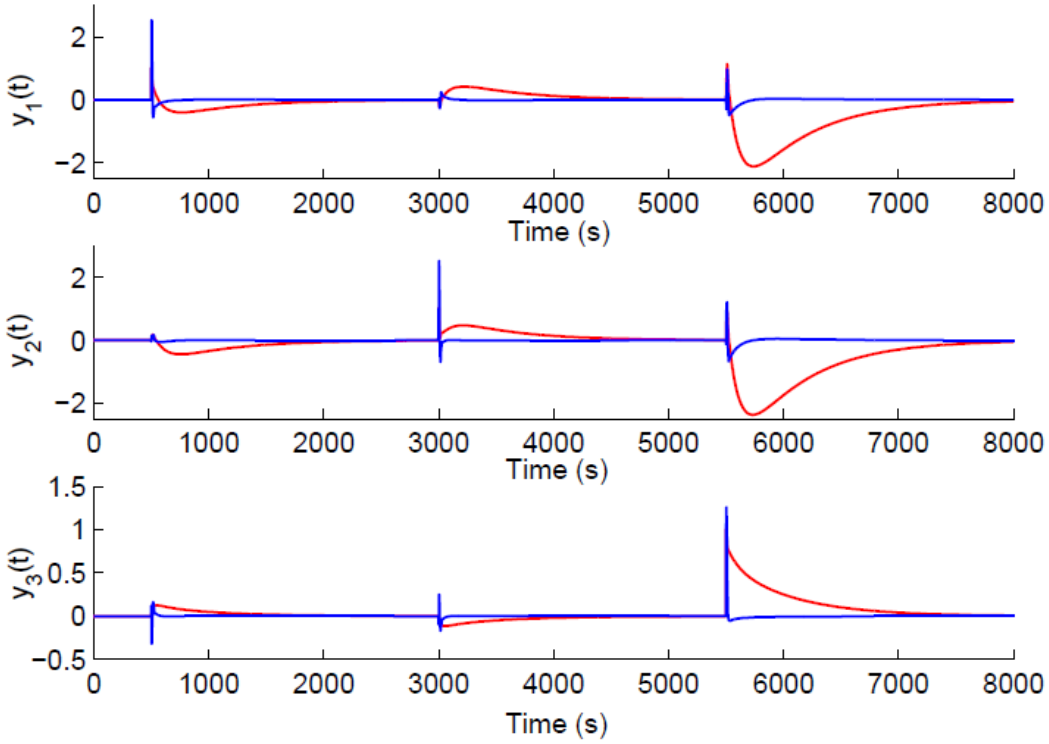

Fig. 15. Disturbance rejection property of the MIMO system without (red line) and with (blue line) feedforward controllers

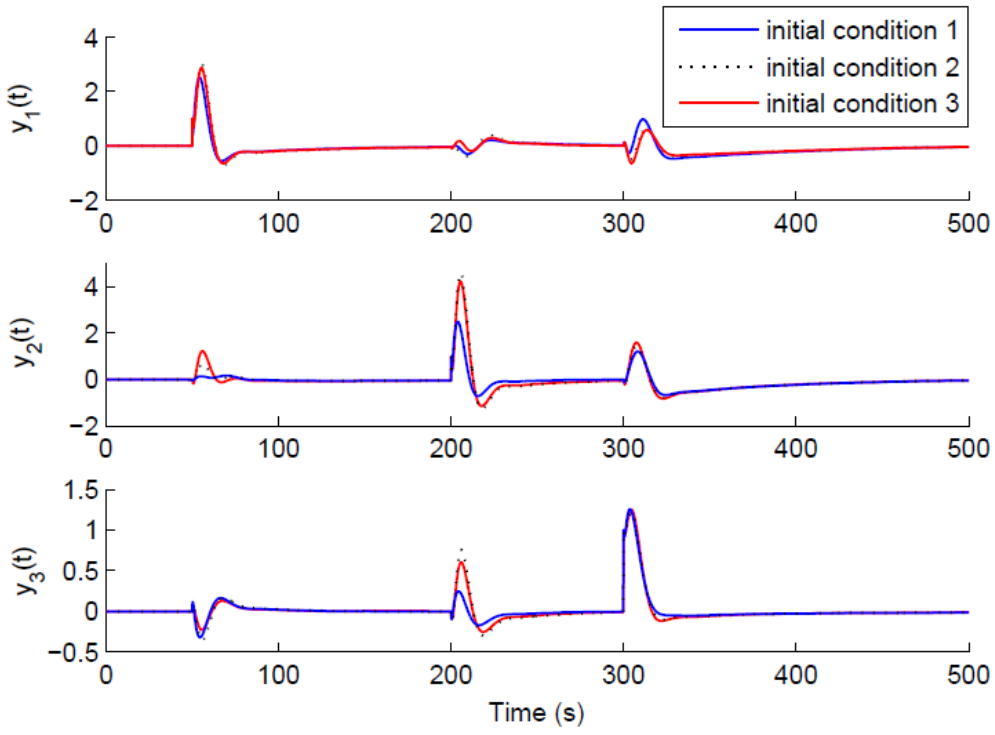

Fig. 16. Disturbance rejection of the system with the feedforward controllers designed using three different initial conditions.

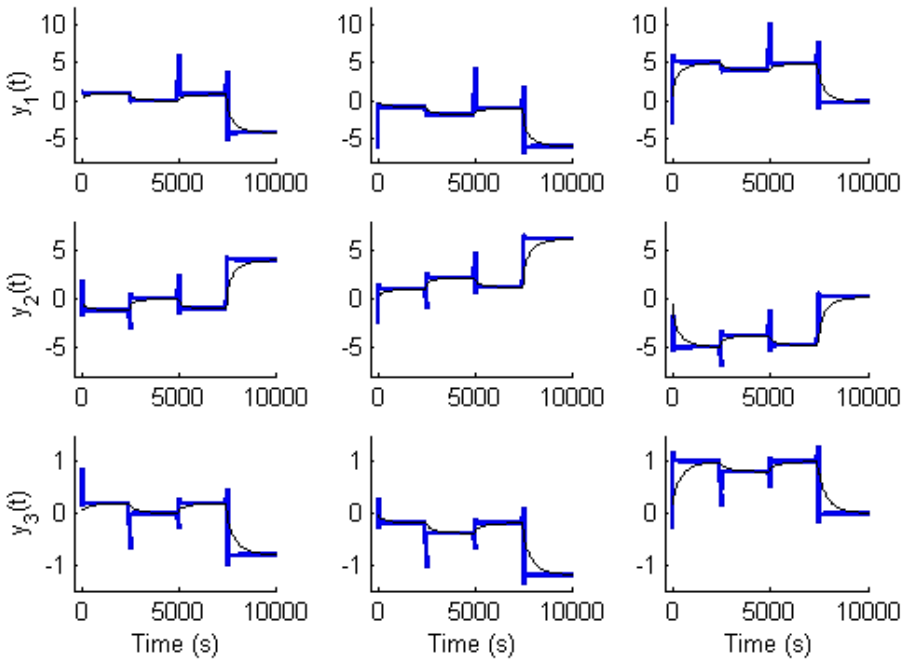

Fig. 17. Control signals without (black line) and with (blue line) employing the feedforward controllers.

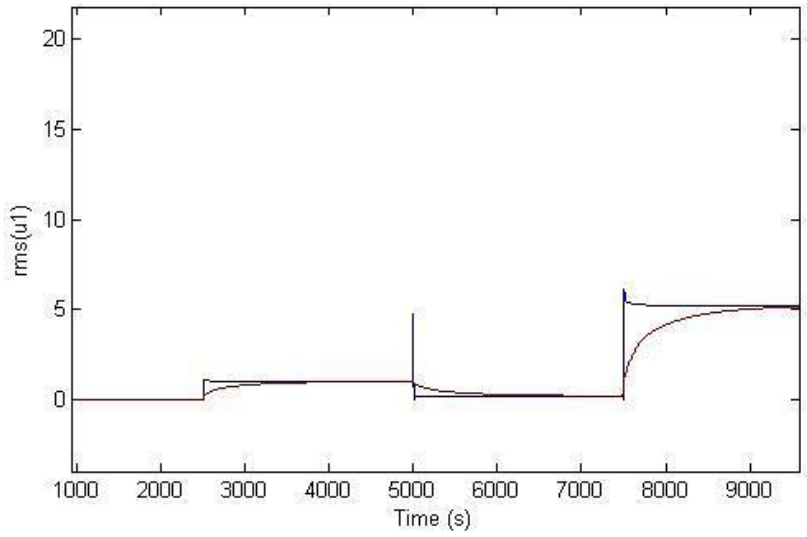

Fig. 18. Comparison between RMS of control signals for the NMP MIMO system with feedforward controller (blue line) and without feedforward controller (red line) for channel 1.

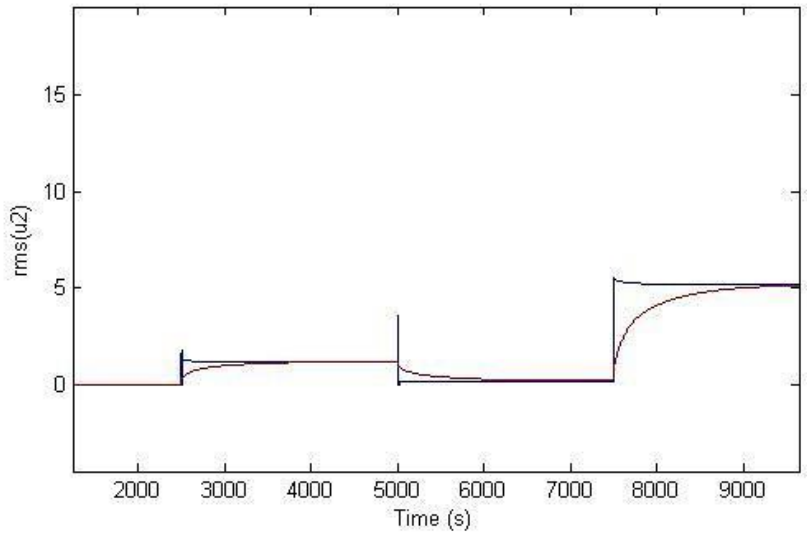

Fig. 19. Comparison between RMS of control signals for the NMP MIMO system with feedforward controller (blue line) and without feedforward controller (red line) for channel 2.

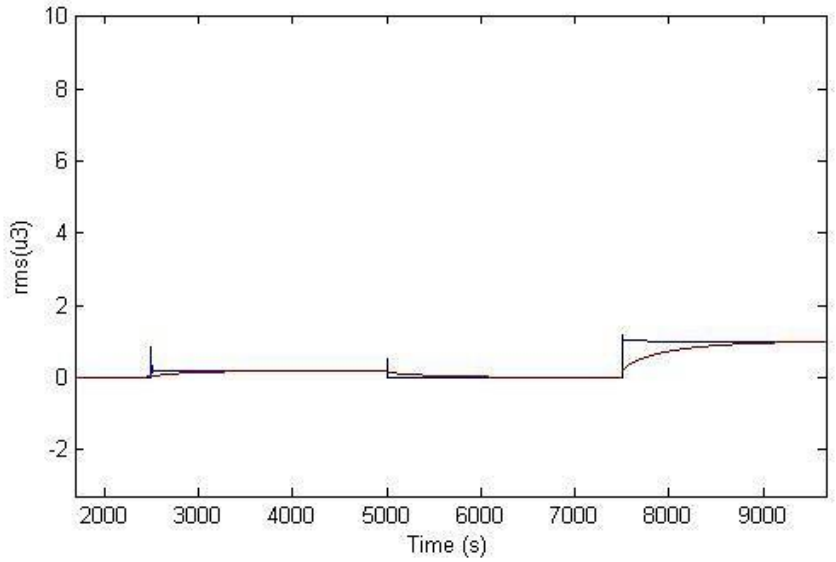

Fig. 20. Comparison between RMS of control signals for the NMP MIMO system with feedforward controller (blue line) and without feedforward controller (red line) for channel 3.

Table 2. Closed-loop performance indices for disturbance rejection.

System	Error	IAE	ISE	ITAE	ITSE
With Feedforward	e_1	140.5184	58.8827	0.55066×10^6	0.58806×10^9
Without Feedforward	e_1	2374.9542	2420.2779	12.075×10^6	80.517×10^9
With Feedforward	e_2	138.382	63.212	0.65078×10^6	1.174×10^9
Without Feedforward	e_2	2645.4945	3017.8395	13.483×10^6	100.41×10^9
With Feedforward	e_3	36.5764	13.1393	0.1624×10^6	0.36435×10^9
Without Feedforward	e_3	495.0434	139.6994	2.467×10^6	4.374×10^9

References

[1] Q. Mei, J. She, Z.-T. Liu, Disturbance rejection and control system design based on a high-order equivalent-input-disturbance estimator, J. Franklin Inst., 358 (2021) 8736-8753.

[2] Y. Du, W. Cao, J. She, M. Wu, M. Fang, Disturbance rejection via feedforward compensation using an enhanced equivalent-input-disturbance approach, J. Franklin Inst., 357 (2020) 10977-10996.

[3] I.M.L.Pataro, J.D. Gil, M.V.A. da Costa, J.L. Guzmán, M. Berenguel, A stabilizing predictive controller with implicit feedforward compensation for stable and time-delayed systems, J. Process Control, 115 (2022) 12-26.

[4] F. García-añas, J.L. Guzmán, F. Rodríguez, M. Berenguel, T. Hägglund, Experimental evaluation of feedforward tuning rules, Control Eng. Pract., 114 (2021) 104877.

[5] W.L. Luyben, Comparison of additive and multiplicative feedforward control, J. Process Control, 111 (2022) 1-7.

[6] Y. Hamada, Flight test results of disturbance attenuation using preview feedforward compensation, IFAC-PapersOnLine, 50 (2017) 14188-14193.

[7] D. Carnevale, S. Galeani, M. Sassano, Transient optimization in output regulation via feedforward selection and regulator state initialization, IFACPapersOnLine, 50 (2017) 2405-8963.

[8] Y. Du, W. Cao, J. She, M. Wu, M. Fang, Disturbance rejection via feedforward compensation using an enhanced equivalent-input-disturbance approach, J. Franklin Inst., 357 (2020) 10977-10996.

[9] S. Liu, G. Shi, and D. Li, Active Disturbance Rejection Control Based on Feedforward Inverse System for Turbofan Engines, IFACPapersOnLine, 54 (2021) 376-381.

[10] D. Tena, I. Peñarrocha-Alós, R. Sanchis, Performance, robustness and noise amplification trade-offs in Disturbance Observer Control design, Eur. J. Control, 65 (2022) 100630.

[11] Y. Ashida, M. Obika, Performance, Data-driven Design of a Feed-forward Controller for Rejecting Measurable Disturbance, Comput. Aided Chem. Eng, 49 (2022) 415-420.

[12] S. Wang, Z. Wu, Z.-G. Wu, Performance, Trajectory tracking and disturbance rejection control of random linear systems, Comput. J. Franklin Inst., 359 (2022) 4433-4448.

[13] G. Shi, S. Liu, D. Li, Y. Ding, Y.Q. Chen, A Controller Synthesis Method to Achieve Independent Reference Tracking Performance and Disturbance Rejection Performance, ACS Omega, 7 (2022) 16164–16186.

[14] Z. Wu, Y. Liu, D. Li, Y.Q. Chen, Multivariable active disturbance rejection control for compression liquid chiller system, Energy, in press (2022) 125344.

[15] Z. Xu, C. Sun, M. Yang, Q. Liu, Active disturbance rejection control for hydraulic systems with full-state constraints and input saturation, Energy, 16 (2022) 1127-1136.

[16] L. Liu, S. Tian, D. Xue, et al, Industrial feedforward control technology: a review, J. Intell. Manuf., 30 (2019) 2819–2833.

[17] S. Tofighi, F. Merrikh-Bayat, A benchmark system to investigate the non-minimum phase behaviour of multi-input multi-output systems, Journal of Control and Decision, 5 (2018) 300-317.

[18] F. Zheng, Q.G. Wang, T.H. Lee, On the design of multivariable PID controllers via LMI approach, Automatica, 38 (2002) 517-526.

[19] S. Boyd, M. Hast, K.J. Astrom, MIMO PID tuning via iterated LMI restriction, Int. J. Robust Nonlinear Control, 26 (2016) 1718-1731.

[20] B. Huang, B. Lu, R. Nagamune, Q. Li, LMI-based linear parameter varying PID control design and its application to an aircraft control system, Aerosp. Syst., 5 (2022) 309–321.

[21] M.N.A. Parlakci, E.M. Jafarov, A robust delay-dependent guaranteed cost PID multivariable output feedback controller design for time-varying delayed systems: An LMI optimization approach, Eur J Control, 61 (2021) 68-79.

[22] Z.Y. Feng, H. Guo, J. She, L. Xu, Weighted sensitivity design of multivariable PID controllers via a new iterative LMI approach, J. Process Control, 110 (2022) 24-34.

[23] J. Sabatier, M. Moze, C.Farges, LMI stability conditions for fractional order systems, Comput. Math Appl., 59 (2010) 1594-1609.

[24] A. Dehak, A.-T. Nguyen, A. Dequidt, L. Vermeiren, M. Dambrine, Reduced-Complexity LMI Conditions for Admissibility Analysis and Control Design of Singular Nonlinear Systems, IEEE Trans. Fuzzy Syst., in press (2022) 1-14.

[25] S. Skogestad, I. Postlethwaite, Multivariable feedback control: analysis and design, 2nd ed., Wiley, New York, 2005.

[26] T. He, G.G. Zhu, X. Chen, A Two-step LMI Scheme for H2- H∞ Control Design, American Control Conference (ACC), Denver, CO, USA, 2020, 1545-1550.

[27] Q. Tran Dinh, S. Gumussoy, W. Michiels, et al, Combining convex-concave decompositions and linearization approaches for solving BMIs, with application to static output feedback, IEEE Trans. Autom. Control, 57 (2012) 1377-1390.

[28] S. Tofighi, F. Merrikh-Bayat, F. Bayat, Robust feedback linearization of an isothermal continuous stirred tank reactor: H∞ mixed-sensitivity synthesis and DK-iteration approaches, Transactions of the Institute of Measurement and Control, 39 (2017) 344-351.

[29] S. Boyd, L.E. Ghaoui, E. Feron, V. Balakrishnan, Linear matrix inequalities in system and control theory, Linear matrix inequalities in system and control theory, 5th ed., SIAM, Philadelphia, 1994.

[30] M. Grant, S. Boyd, CVX: Matlab software for disciplined convex programming, version 2.0 beta, http://cvxr.com/ (2013, accessed March 2022).

[31] R.H. Tutuncu, K. C. Toh, M.J. Todd, Solving semidefinite-quadratic-linear programs using SDPT3, Math Program, 95 (2003) 189-217.

[32] R. Wood, M. Berry, Terminal composition control of a binary distillation column, Chem. Eng. Sci., 28 (1973) 1707-1717.

[33] M. Hovd, M. Skogestad, Simple frequency tools for control system analysis, structure selection, and design, Automatica, 28 (1992) 989–996.

[34] F. Merrikh-Bayat, An iterative LMI approach for H∞ synthesis of multivariable PI/PD controllers for stable and unstable processes, Chem. Eng. Res. Des., 132 (2018) 606–615.

HOW TO CITE THIS ARTICLE

S. Tofighi, F. Merrikh-Bayat, F. Bayat, Disturbance rejection of non-minimum phase MIMO systems: An iterative tuning approach, AUT J. Model. Simul., 54(2) (2022) 141-160.

DOI: 10.22060/miscj.2022.21598.5291